Journal of the Korean Magnetic Resonance Society **2023**, *27*, 35-41
DOI 10.6564/JKMRS.2023.27.4.035

Four New Furanosesquiterpenes Isolated from the Marine Sponge *Dysidea* species

Yeong Du Yoo and Jung-Rae Rho*

Department of Oceanography, Kunsan National University, Gunsan 54150, Republic of Korea

Received Dec 14, 2023; Revised Dec 18, 2023; Accepted Dec 18, 2023

Abstract From a marine sponge *Dysidea* species, four new furanosesquiterterpenoids were isolated and characterized. Their structural elucidation was achieved through an extensive analysis employing NMR, MS data, and DFT method. Notably, all compounds shared as identical molecular formula. Compound **2** was identified as a derivative of compound **1**, while compounds **3** and **4** exhibited an identical planar structure. Determination of the configurations of chiral centers in compounds **1** and **2** involved a comparative analysis between measured and calculated ECD spectra, along with the application of DP4+ probability analysis. Distinctly, the configurations of isomers **3** and **4** were established by scrutinizing proton chemical shifts based on the NOE correlation.

Keywords 1D and 2D NMR, *Dysidea* sp, DFT method, DP4+ probability, configuration determination

Introduction

Furanosesquiterpenes, known for their diverse chemical structures, have been isolated from both terrestrial and marine organisms.[1,2] These compounds exhibit a broad spectrum of biological effects, ranging from cytotoxic and antifungal properties to anti-inflammatory actions, antiviral activities, and induction of HIV apoptosis.[3,4] In our quest to uncover bioactive compounds from Korean Marine sponges,[5,6] four new furanosesquiterpenes were isolated from *Dysidea* sp. Initially guided by NO inhibitory activity, the process of fractionation and isolation were conducted. However, these four isolated compounds did not demonstrate any NO-inhibitory effect or cytotoxicity.

Determining the planar structures of these compounds involved a combination of 1D and 2D NMR spectra and establishing configurations of their chiral centers relied on employing the DFT (density functional theory) method. Theoretical calculations, primarily through DFT methods, have proved remarkably effective in predicting nuclear chemical shifts, and coupling constants, and ECD (electron circular dichroism) spectra.[7,8] These methodologies have served as a solution for determining the relative or absolute configurations of natural products for decades.[9] The determination of the configurations of natural products has presented a challenging problem in structure elucidation. The enantiomers of chiral centers in natural products or drugs may exhibit significantly different biological and pharmacological behaviors within chiral living systems.

This paper details the isolation of compounds **1**–**4** from a marine sponge *Dysidea* sp. Subsequently, based on the determined planar chemical structures via a combination of NMR and MS experiments, the assignment of configurations for their chiral centers was investigated by the application of DFT methods

* Address correspondence to: **Jung-Rae Rho,** Department of Oceanography, Kunsan National University, Gunsan 54150, Republic of Korea, Tel: 82-63-469-4606; Fax: 82-63-469-7441; E-mail: jrrho@kunsan.ac.kr

and the difference in proton chemical shifts of isomers.

Experimental Methods

*Extraction and Isolatio*n - In 2010, a marine sponge *Dysidea* sp. (sample no. 10G-5) was manually collected using SCUBA equipment from Gage island. The freeze-dried specimen, weighing 10.5 Kg, underwent two methanol (MeOH) extraction at room temperature. Initially, the crude extract was partitioned between H_2O and methylene chloride (MC), followed by a secondary partitioning of the MC layer between hexane and 15% aqueous MeOH to eliminate fatty acids. The resulting polar fraction then underwent reversed-phase vacuum flash chromatography, employing stepwise gradients of MeOH in H_2O (50%, 60%, 70%, 80%, 90%, 100%).
The 80% MeOH fraction, revealing promising signals in the low-field region of the ^1H NMR spectrum, underwent further separation into five subfraction (M1–M5) using Sephadex LH20 open column chromatography to facilitate effective compound isolation. Among these, the M5 fraction (120 mg), exhibiting the targeted signals, underwent separation via reversed-phase HPLC (YMC ODS-A column, 250mm × 10mm, Varian RI detector) utilizing a solvent system (H_2O/MeOH=33/67), resulting in the separation of compounds **1**-**4**. Compound **1** (4 mg), **2** (5.4 mg), **3** (4.8 mg) and 4 (4.7 mg) were purified with retention times of 33, 27, 29, and 36 minutes, respectively.

NMR experiments - The 1D and 2D NMR spectra were acquired using a Varian NMR system operating at 500 MHz for proton and 125 MHz for carbon nuclei. Chemical shifts for ^1H and ^{13}C NMR spectra were referenced to CD_3OD at 3.30 and 49.0 ppm, respectively. Throughout all experiments, the temperature was maintained at a constant 297 K.
Specific parameters for the 2D NMR experiments were as follows: Gradient COSY spectra were gathered within a spectral width of 2567 Hz using a 512(t1) × 1024 (t2) matrix, employing a 1 ms pulse gradient with a strength 10 G/m. These spectra were processed using a sinebell function for optimal results. For the gradient HSQC spectra, measurements were conducted in a 128(t1) × 1024(t2) matrix, utilizing J_{CH}=140 Hz and processed in a 256 (t1) × 1024(t2) matrix through a linear prediction method to achieve higher resolution.
The gradient HMBC experiment was fine-tuned for a long-range coupling constant of 8 Hz. Additionally, the NOESY experiment involved a mixing time of 250 *ms* to capture pertinent data for analysis.

Results and Discussion

The 20% aqueous MeOH fraction obtained from the extract underwent LH20 open column chromatography, yielding five fractions (M1–M5). Among these, the M5 fraction was further purified using reversed-phase HPLC, resulting in the isolation of compounds **1**-**4**, identified as new furanosesquiterpenes (Figure 1). Elucidation of the planar structure of all compounds involved a comprehensive analysis integrating NMR and MS experiments. Subsequently, the configurations of the chiral centers were precisely determined employing the DFT method alongside an analysis of proton chemical shifts.

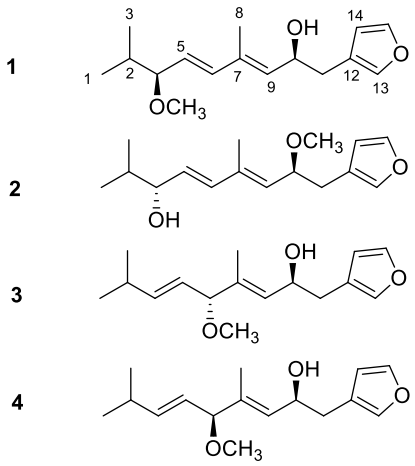

Figure 1. Four compounds isolated from the marine sponge *Dysidea* sp.

Compound **1** was isolated as a colorless oil and given as a molecular formula $C_{16}H_{24}O_3$ based on the sodium-adducted ion peak ($[M+Na]^+$ *m*/*z* = 287.1628, Δ=3.6 ppm) of the HR-ESI MS spectrum. The ^1H and ^{13}C NMR spectra measured in CD_3OD showed the four methyls including a methoxy moiety and six olefinic proton signals in the downfield region. Together with 1D NMR data, careful analysis of COSY NMR spectra showed that **1** contained the three partial substructures A~C, as shown in Figure 2.

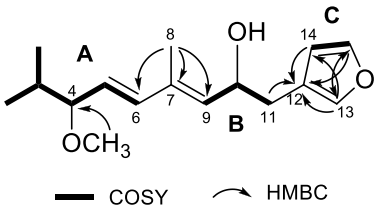

Figure 2. COSY correlations and Key HMBC correlations of **1**.

Furthermore, the HMBC correlations from the methyl proton at δ_H 1.70 to three carbons at δ_C 135.5 (C-9), 135.6 (C-7), and 139.1 (C-6) constructed a monoterpene from the linkage of the two substructures A and B. The olefinic proton at δ_H 7.28 (H-13) was correlated with the carbons at δ_C 112.7 (C-14) and 143.7 (C-15), and the proton at δ_H 7.34 (H-15) was correlated with the carbons at δ_C 122.2 (C-12) and 141.4 (C-13) in the HMBC spectrum, suggesting the presence of a furan ring based on the molecular formula. Additional HMBC correlations of H-11, H-13, and H-14 with C-12 connected substructures C with B, establishing **1** as a sesquiterpene skeleton. The remaining two oxygens were attached to C-4 and C-10 from their carbon chemical shifts. Moreover, the methoxy unit was determined to be connected to C-4 by the HMBC correlation of the methoxy protons and C-4. The geometry of the two double bonds were assigned as *E* form based on a large proton coupling constant ($^3J_{5,6}$ = 15.7 Hz) and the NOESY cross peak between H_3-8 and H-10. Furthermore, the main conformation from C-4 to C10 of **1** could be proposed as Figure 3, based on the large coupling constants ($^3J_{5,6}$ = 8.1 Hz, $^3J_{9,10}$ = 8.6 Hz) and the NOE cross peaks of H_3-8/H-10, H-4/H-6, and H-6/H-9. However, the configurations of the two chiral centers (C-4 and C-10) could not be determined solely through NOE correlations. Instead, comparison between calculated and measured ECD spectra (shown in Figur 4) led to determine the two configurations of **1**. For this, four isomers of **1** were initially labeled as 4*R*10*R*, 4*S*10*R*, 4*R*10*S*, and 4*S*10*S*. The low-energy conformations for each isomer were found based on a method outlined in Ref. 10.

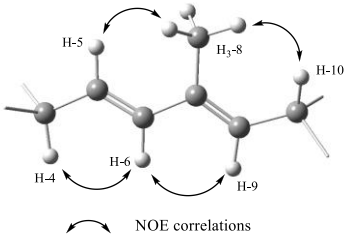

Figure 3. NOESY correlations in **1**.

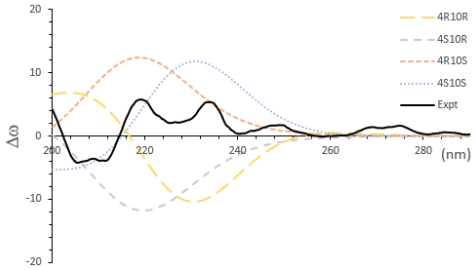

Figure 4. Measure and calculated ECD spectra in **1**.

Among these conformations, those aligning well with the observed coupling constants and NOE correlations were selected. For each isomer, subsequent calculations of the ECD spectra for the chosen conformations were performed using the DFT method at the B3LYP/6-31G(d,p)//M062X /6-31G(d,p) level with PCM. The resulting ECD spectrum, weighted by Boltzmann distribution, was obtained. While the measured ECD spectrum showed weak signal, it demonstrated relatively close agreement with that of the 4*S*10*S* isomer rather than the 4*R*10*S* isomer. In order to substantiate the greater likelihood of the 4*S*10*S* isomer over the 4*R*10*S* isomer, the DP4+ probability method,[11,12] utilized for determining probabilities of various proposed

chemical structures based on experimental NMR data, was employed. Initially, theoretical NMR chemical shifts for both isomers were calculated using DFT method at the MPW1PW91/6-311G(d,p)//M062X/6-31G(d,p) level with PCM for the above selected conformations. Subsequently, the DP4+ probability was found to be 100% for the 4*S*10*S* isomer. As a result, the compound **1** was determined to possess the 4*S*10S configuration based on both quantum calculations.

Compound **2** was provided with the same molecular formula as compound **1**. While compound **2** exhibited the ^{1}H and ^{13}C NMR spectra similar to those of **1**, several signals in the intermediate spectrum region were notably shifted. For instance, the proton signal at δ_H 3.33 (H-4) in **1** shifted to a low field at δ_H 3.82 in **2**, while the signal δ_H 4.59 (H-10) shifted to a high field at δ_H 4.22. Analysis of 1D and 2D NMR spectra of **2** revealed a chemical structure highly resembling **1**, except for the positional change of the methoxy group. It is deduced that the methoxy group was attached at C-10 based on the HMBC correlation between the methoxy proton at δ_H 3.23 and the carbon at δ_C 78.8 (C-10). Similarly to compound **1**, the configurations of the two chiral centers of **1** were determined by comparing the calculated and measured ECD spectra. Interestingly, the ECD spectrum of **2** closely resembled that of **1** but leaned towards the calculated 4*R*10*S* isomer of **2**, as depicted in the Figure 5.

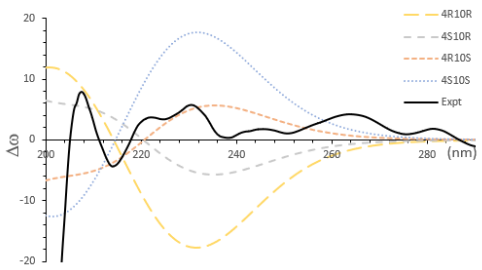

Figure 5. Measure and calculated ECD spectra in **2**.

Similar to the previous case, the DP4+ probability method was utilized for both 4*R*10*S* and 4*S*10*S* isomers of compound **2**. The DP4+ probability for the 4*R*10*S* isomer yielded a 100% match, aligning with the result from ECD spectra. Accordingly, the compound **2** was determined to possess the 4*R*10*S* configuration.

Compound **3** and **4** showed an identical molecular formula with the proceeding two compounds. While their carbon chemical shifts differed by less than 0.01 ppm, notable distinctions emerged in proton chemical shifts, particularly in H-4 and the methoxy protons (Figure 8). Analysis of the COSY and HMBC NMR spectra elucidated the same planar structure shown in Figure 6.

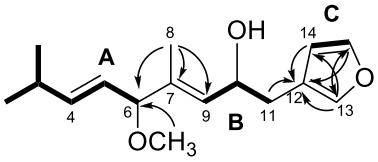

Figure 6. COSY correlations and Key HMBC correlations of **3** and **4**.

Compared to compound **1**, the position of a double bond ($^{4,5}\Delta$) and the methoxy groups were changed. Characteristic aspect in compounds **3** and **4** was that, in compound **3**, the H-4 exhibited a lower field shift compared to compound **4**, whereas the methoxy protons in **3** experienced a higher field shift than in **4**. The NOESY spectra in compounds **3** and **4** showed a shared structure framework, as illustrated in Figure 7.

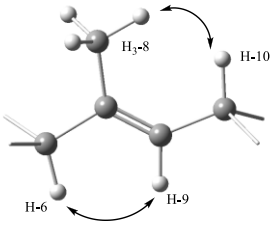

Figure 7. NOESY correlations in **3** and **4**.

Moreover, considering similar carbon and proton chemical shifts from C-9 to C-15 in compounds **1**, **3**, and **4**, C-10's configuration was determined as 10*S*. However, differing proton chemical shifts in H-4 and methoxy group indicated varying configurations of the chiral enter (C-6). The energy-minimized molecular models for the 4*R* and 4*S* isomers highlighted differences in the proton chemical shifts

for H-4 and methoxy protons. As depicted in Fig. 5, methoxy protons in the 4*R* isomer were directed toward the aromatic furan ring, inducing a high-field shift due to ring current. Conversely, the double bond group in the 4*S* isomer directed toward the furan ring and exhibited a high-field shift. Consequently, the 4*R* isomer with a smaller proton chemical shift in the methoxy group was designated as compound **3**, while the 4*S* isomer with a smaller value in the double bond was assigned as compound **4**.

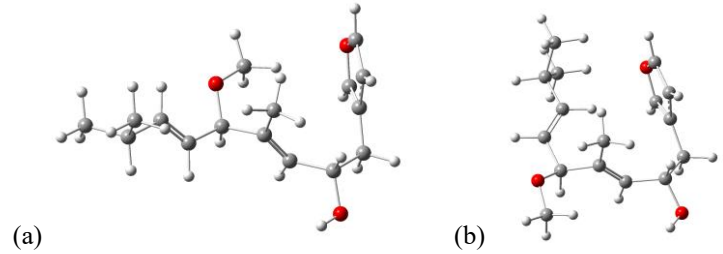

Figure 8. Energy-minimized structures of (a) **4*R*** and (b) **4*S*** isomer.

Table 1. Spectral data for compounds **1**– **4** in CD_3OD (500 MHz for ^1H, 125 HMz for ^{13}C).

	1		**2**	
position	δ_C, mult	δ_H (*J* in Hz)	δ_C, mult	δ_H (*J* in Hz)
1	18.7, CH_3	0.85, d(6.9)	18.6, CH_3	0.91, d(6.9)
2	34.1, CH	1.74, m	35.4, CH	1.69, m
3	19.0, CH_3	0.92, d(6.9)	18.7, CH_3	0.91, d(6.9)
4	89.4, CH	3.33, m	78.9, CH	3.82, t(7.1)
5	128.5, CH	5.45, dd(15.7, 8.1)	131.6, CH	5.65, dd(16.7, 7.1)
6	139.1, CH	6.19, d(15.7)	136.1, CH	6.22, d(16.7)
7	135.6, CH	-	138.3, CH	-
8	13.1, CH_3	1.70, d(1.0)	13.3, CH_3	1.71, d(1.0)
9	135.5, CH	5.47, d(8.6)	132.8, CH	5.30, d(9.3)
10	69.4, CH	4.59, dt(8.6, 6.6)	78.8, CH	4.22, dt(9.3, 6.6)
11	34.0, CH_2	2.57, dd(14.2, 6.6)	31.9, CH_2	2.54, dd(14.4, 6.6)
		2.69, dd(14.2, 6.6)		2.73, dd(14.4, 6.6)
12	122.2, C	-	122.2, C	
13	141.4, CH	7.28, br s	141.3, CH	7.26, br s
14	112.7, CH	6.31, br d(1.7)	112.7, CH	6.30, br d(1.7)
15	143.7, CH	7.34, d(1.7)	143.7, CH	7.35, t(1.7)
4-OCH_3	56.6, CH_3	3.23, s		
6-OCH_3				
10-OCH_3			56.2, CH_3	3.23, s
	3		**4**	
ποσιτιον	δ_C, mult	δ_H (*J* in Hz)	δ_C, mult	δ_H (*J* in Hz)
1	22.7, CH_3	0.96, d(6.9)	22.7, CH_3	0.99, d(6.9)
2	32.1, CH	2.28, hd(6.9, 0.7)	32.1, CH	2.26, hd(6.9, 0.7)
3	22.7, CH_3	0.96, d(6.9)	22.7, CH_3	0.99, d(6.9)
4	141.5, CH	5.63, ddd(15.7, 6.9, 1.2)	141.4, CH	5.56, ddd(15.7, 6.9, 1.2)
5	127.1, CH	5.29, ddd(15.7, 6.6, 1.5)	127.2, CH	5.28, ddd(15.7, 6.6, 1.5)
6	88.4, CH	3.88, d(6.6)	88.4, CH	3.90, d(6.6)
7	137.8, C	-	138.0, C	-
8	12.4, CH_3	1.45, d(1.2)	12.1, CH_3	1.44, d(1.2)
9	131.2, CH	5.42, br d(8.8)	131.4, CH	5.41, br d(8.8)
10	69.1, CH	4.50, ddd(8.8, 7.6, 6.1)	69.2, CH	4.49, ddd(8.8, 7.6, 5.9)
11	34.0, CH_2	2.53, dd(13.9, 7.6)	34.0, CH_2	2.51, dd(14.2, 7.6)
		2.72, dd(13.9, 6.1)		2.69, dd(14.2, 5.9)
12	122.1, C	-	122.1, C	-
13	141.4, CH	7.28, br s	141.4, CH	7.25, br s
14	112.7, CH	6.33, br d(1.7)	112.8, CH	6.30, br d(1.7)
15	143.7, CH	7.36, t(1.7)	143.6, CH	7.35, t(1.7)
4-OCH_3				
6-OCH_3	55.9, CH_3	3.11, s	56.0, CH_3	3.16, s

10-OCH_3

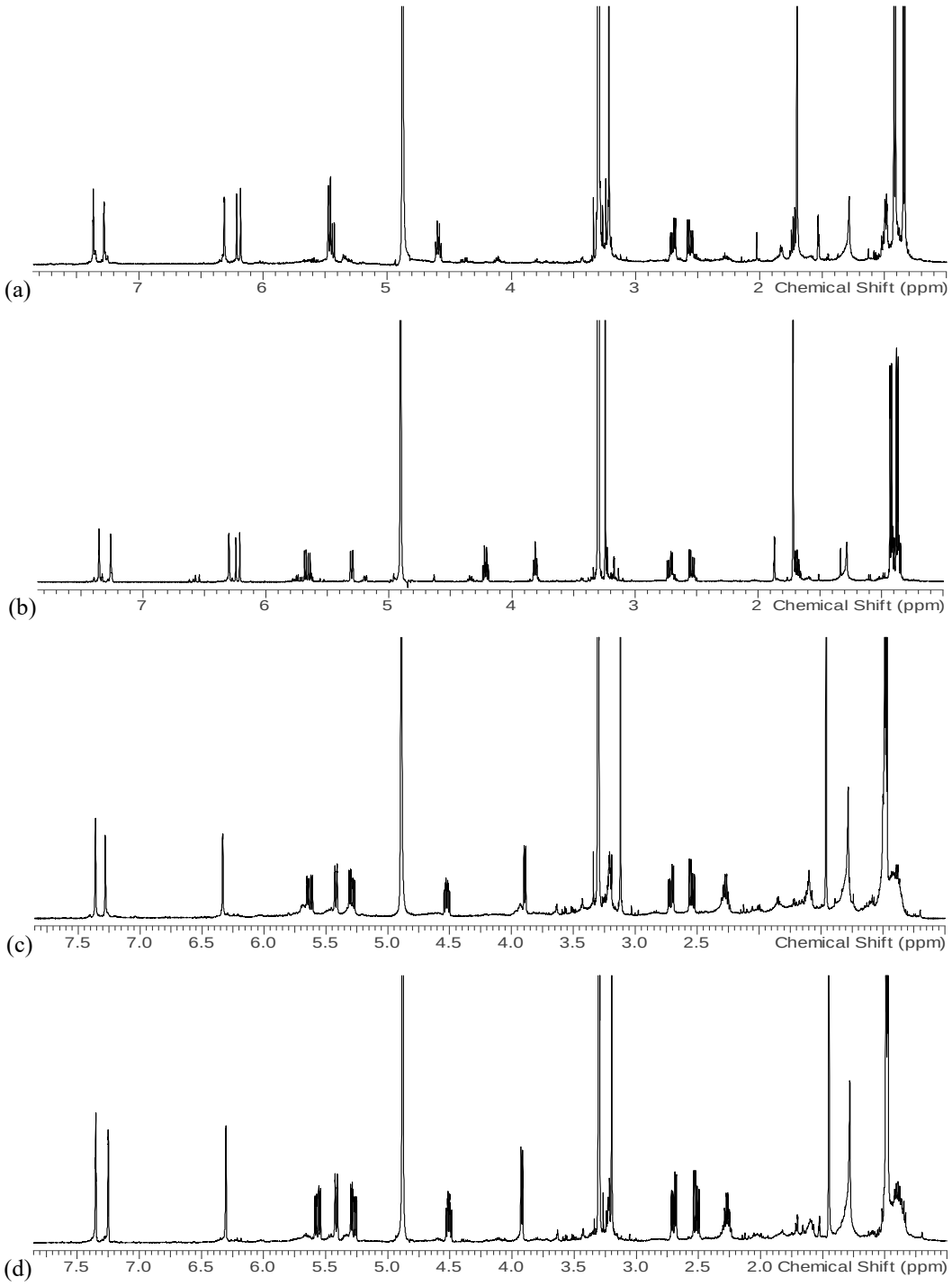

Figure 9. ^{1}H NMR spectra of (a) compound **1**, (b) **2**, (c) **3**, and (d) **4**.

Acknowledgements

This research was supported by “Regional Innovation Strategy (RIS)” through National Research Foundation of Korea (NRF) funded by the ministry Education (MOE) (2023RIS-008) and Korea Institute of Marine Science & Technology (KIMST) funded by the Ministry of Oceans and Fisheries (RS-2023-00256330, Development of risk managing technology tackling ocean and fisheries crisis around Korean Peninsula by Kuroshio Current).

References

1. S. Rajaram, U. Ramulu, D. Ramesh, D. Srikanth, P. Bhattacharya, P. Prabhakar, S. V. Kalivendi, K. S. Babu, Y. Venkateswarlu, S. Navath, *Bioorg. Med. Chem. Lett.* **23**, 6234 (2013)
2. T. Gyeltshen, B. J. Deans, C. C. Ho, N. L. Kilah, J. A. Smith, A. C. Bissember, *J. Nat. Prod.* **86**, 1584 (2023)
3. H. N. Kamel, M. Slattery, *Pharm. Biol.* **43**, 243 (2005)
4. S. Y. Cheng, K. J. Huang, S. K. Wang, Z. W. Wen, P. W. Chen, C. Y. Duh, *J. Nat. Prod.* **73**, 771 (2010)
5. S. Y. Park, B. S. Hwang, K. H. Ji, J-R. Rho, *J. Kor. Magn. Reson.* **11**, 122 (2007)
6. B. S. Hwang, Y. T. Jeong, S. Lee, E. J. Jeong, J-R. Rho, *Molecules* **26**, 3164 (2021)
7. J. Vaara, J. Jokisaari, R. E. Wasylishen, D. L. Bryce, *Prog. Nucl. Magn. Reson. Spectrosc*. **41**, 233 (2002)
8. G. Pescitelli, L. D. Bari, N. Berova, *Chem. Soc. Rev*. **40**, 4603 (2011)
9. W. S. Brickell, S. F. Mason, D. R. Roberts, *J. Chem. Soc. B* 691 (1971)
10. W. Hehre, P. Klunzinger, B. Deppmeier, A. Driessen, N. Uchida, M. Hashimoto, E. Fukushi, Y. Takata, *J. Nat. Prod.* **82**, 2299 (2019)
11. N. Grimblat, M. M. Zanardi, A. M. Sarotti, *J. Org. Chem*. **80**, 12526 (2015)
12. A. Bagno, F. Rastrelli, G. Saielli, *Chem. Eur. J.* **12**, 5514 (2006)